Remote Sensing and Machine Learning-Driven Flood Inundation Mapping of September 2025 Ravi Watershed Using Sentinel-1 SAR

Bareera Bilal, Rania Saleemi, Areeba Amer, Hamid Gulzar
Institute of Space Science, University of the Punjab, Lahore, Pakistan
*Correspondence: geotechs49@gmail.com

Citation | Bilal. B, Saleemi. R, Amer. A, Gulzar. H, "Remote Sensing and Machine Learning-Driven Flood Inundation Mapping of September 2025 Ravi Watershed Using Sentinel-1 SAR", IJIST, Vol. 07 Issue. 04 pp 2346-2358, October 2025
Received | August 28, 2025 **Revised |** October 5, 2025 **Accepted |** October 7, 2025 **Published |** October 9, 2025.

Floods is among the most devastating natural hazards in South Asia. The September 2025 flood in the Ravi Basin was triggered by heavy monsoon rainfall and the release of water from cross-border dams. This study utilized Sentinel-1 SAR data, including both ascending and descending passes in VH polarization, to map flood inundation across the basin using a Random Forest classifier. Pre-flood and post-flood composites were prepared for April-May and 27 August to 5 September, respectively. The predictors feature includes VH_pre, VH_post, VH_diff, and VH_ratio. Terrain correction using the NASA DEM and landcover filtering with ESA WorldCover at 10m improved classification accuracy. Results showed that 1,885 km² of land was inundated, representing 5% of the total basin area. Approximately 260 settlements were impacted, including Dera Baba Nanak, Kartarpur, and the low-lying regions of Lahore. Croplands were the most affected class, with 1,610 km² flooded, followed by grasslands (90 km²) and sparse vegetation (62 km²). Built-up areas accounted for 0.7 km² of inundation, though the socio-economic impact was disproportionately high. Precipitation analysis from NOAA CPC confirmed rainfall clustering in the Sialkot and Narowal corridor. The peaks exceeding 800 mm/day cause this region as the epicenter of the flood. News reports corroborated satellite findings, noting that over 2.5 million displaced and more than 100 lives were lost. The study highlights how tributary floods involving the Ravi, Sutlej, and Chenab are emerging as severe hazards for Punjab. Findings underline the need for improved monitoring, resilient agricultural strategies, and disaster preparedness to mitigate future economic and food security risks.

Keywords: Flood Mapping, Sentinel-1 SAR, Random Forest, Remote Sensing, Punjab, Pakistan

Introduction:

In the 21st century, disasters have become a significant challenge, impacting societies and economies on a large scale [1]. Among various hazards, floods are considered the most destructive, causing substantial economic losses and numerous human casualties worldwide [2][3][4]. Rapid urbanization, population growth, and the intensification of climate change are increasing community vulnerability to flooding events [5]. The Intergovernmental Panel on Climate Change (IPCC) has consistently highlighted that global warming intensifies the hydrological cycle, leading to increased rainfall extremes and more frequent high-magnitude flood events [6][7]. This highlights the urgent need for reliable monitoring systems to provide timely flood information for preparedness, response, and adaptation. Climate change is increasingly associated with altered precipitation patterns, glacier retreat, and rising sea levels, all of which amplify flood risk [8][9][10][11][12]. Recent studies indicate that warming-induced changes in monsoon dynamics and convective storms are generating extreme rainfall events in both humid and arid regions [13][14][15]. Such extremes are particularly evident in South Asia, where densely populated river basins such as the Indus, Ganges, and Brahmaputra frequently experience devastating floods [16][17][18][19]. Flooding can result from various factors, including heavy rainfall, snowmelt, glacial lake outburst floods (GLOFs), and river overflows, with its impacts influenced by topography, land use, and socio-economic exposure [20][21]. The 2020 floods in Bangladesh and India and the 2022 floods in Pakistan highlight how climatic variability drives large-scale humanitarian crises [17][22][23][24]. The September 2025 floods in Pakistan stand out as a major event requiring a detailed scientific assessment. Severe monsoon rains have triggered high to medium flooding in rivers and nullahs across Punjab [25]. Flooding led to the evacuation of over 200,000 people from low-lying areas [26]. For the first time, simultaneous flooding was recorded in three major rivers: the Ravi, Sutlej, and Chenab[27]. The precipitation spell began on August 15 and lasted until September 10, with a peak of 364 mm recorded within just 24 hours in the upper Punjab region [28]. Remote sensing has revolutionized flood monitoring by providing spatially consistent and temporally repeatable observations over large areas [29]. Optical sensors such as Landsat and Sentinel-2 are widely used for flood mapping through indices like NDWI and MNDWI; however, their effectiveness is often limited by persistent cloud cover during flood events [30][29][31][15][32]. The same limitation affected the use of optical data during the study event. In contrast, microwave sensors, particularly Synthetic Aperture Radar (SAR), overcome these challenges as they operate independently of sunlight and weather conditions. [31]. SAR data allow the detection of smooth water surfaces due to their low backscatter, making them a preferred choice for flood mapping [33].

Several methodologies are employed for flood detection using SAR, including traditional approaches such as backscatter histogram thresholding, change detection between pre- and post-event images, and supervised classification techniques [4]. More advanced techniques utilize interferometric coherence to detect surface changes caused by inundation [33][34], while hybrid frameworks that integrate thresholding, object-based analysis, and region-growing algorithms offer improved accuracy [35][36]. Automatic thresholding methods, such as Otsu's algorithm, have been effectively implemented on cloud-based platforms like Google Earth Engine for rapid flood assessment [37]. Case studies in Namibia, Bangladesh, and India further demonstrate the robustness of these techniques for operational applications [16][38][39][23]. SAR backscatter is highly sensitive to surface roughness and dielectric properties, enabling the delineation of open water and inundated vegetation alike [40]. The free availability of Sentinel-1 SAR data has enabled large-scale, near-real-time flood monitoring, even in data-scarce regions [34]. Taken together, these advantages make SAR an indispensable component of modern flood risk assessment frameworks. This study specifically aims to map the September 2025 flood in the Ravi Basin (Figure 1), a critical sub-catchment of the Indus River in Pakistan. The Ravi basin, which sustains agriculture, major settlements have experienced extensive inundation during this event [41]. The objectives of the study are: (i) to employ SAR-based methodology for precise delineation of flood extent; (ii) to assess the spatial distribution of inundation across different land-use categories. By focusing on this event, the research not only contributes to the scientific understanding of climate-driven flood hazards but also supports policy frameworks for disaster resilience in Pakistan and the wider South Asian region.

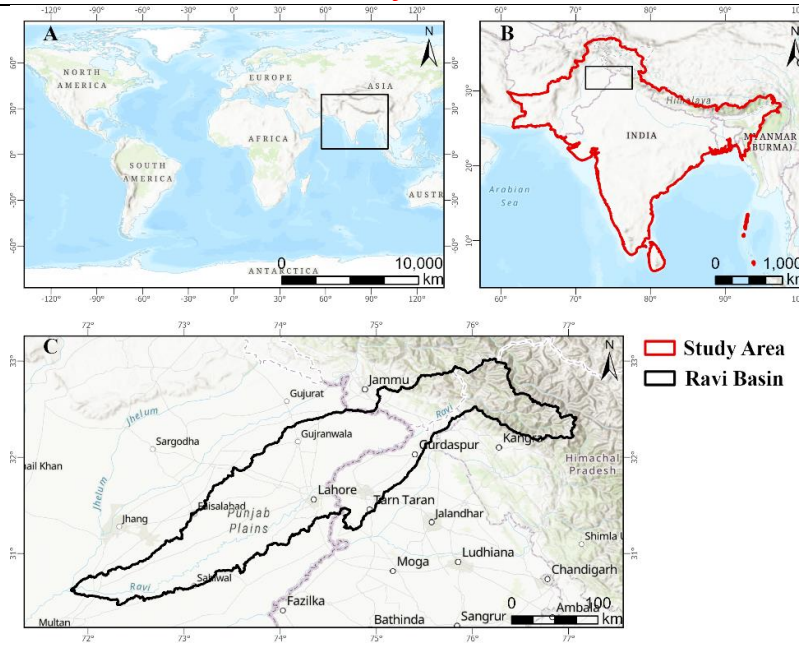

Figure 1. Study area map of the Ravi River basin (C) and its locators (A, B)

Methodology:

Data Collection:

This study employed Sentinel-1 synthetic aperture radar (SAR) data at 10m spatial resolution for mapping flood extents in the Ravi Basin during the September 2025 flood event. Both ascending and descending pass images in VH polarization were acquired in Interferometric Wide (IW) swath mode from the Google Earth Engine (GEE) repository. Two temporal windows were defined: a pre-flood reference period spanning April to May, and a flood period from August 27 to September 4. Mean backscatter composites were derived for each pass under both pre-flood and post-flood conditions. The ascending and descending composites were subsequently processed separately and later merged to enhance spatial coverage and minimize geometric distortions. Figure 2 and Table 1 present the locations and acquisition dates of both passes.

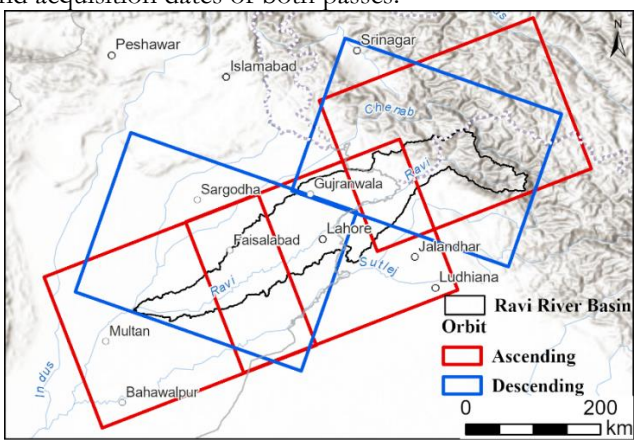

Figure 2. Coverage of Sentinel-1 satellite orbits over the Ravi River Basin.

Table 1. Sentinel-1 ascending and descending acquisitions over the Ravi Basin during late August–early September 2025, showing coverage of upper, middle, and lower reaches.

Orbit Direction	Acquisition Date	Coverage Area
Ascending	27 August 2025	Middle Ravi Basin
	01 September 2025	Lower Ravi Basin
	03 September 2025	Upper Ravi Basin
Descending	28 August 2025	Lower Ravi Basin
	04 September 2025	Upper Ravi Basin

From these composites, additional predictor layers were derived, including the pre-flood VH (VH_pre), post-flood VH (VH_post), difference (VH_diff), and ratio (VH_ratio). These bands were combined into a multi-band composite, which served as the input feature stack for classification (Figures 3 and 4). In the pre-/post-flood stack, red areas indicate flooding, while black to dark blue areas represent permanent water bodies. Based on this spectral response, training regions of interest (ROIs) were manually digitized for two main classes: flooded and non-flooded areas, with additional ROIs used to mark permanent water bodies. A total of 300 ROIs (150 per class) were sampled across different parts of the basin to ensure representativeness. A Random Forest classifier with 50 decision trees was then trained and applied to generate the flood classification map. To reduce false positives, terrain correction was integrated using NASA's SRTM-derived DEM. Pixels in areas with slopes greater than 45° were masked to eliminate steep-terrain errors caused by SAR shadow effects, ensuring that the classification remained confined to plausible floodplain zones. Similarly, snow and ice regions were removed using ESA WorldCover 2020 data, thereby constraining flood detection to lowland areas. The resultant 10 m resolution flood mask was further intersected with land cover to estimate inundated croplands and urban settlements. Accuracy assessment was performed using an independent set of validation ROIs, yielding an overall accuracy of 98.3% and a Kappa coefficient of 0.97, confirming the robustness of the classification. In addition, OpenStreetMap (OSM) settlement data were overlaid with the flood extent, allowing estimation of settlements directly affected by inundation.

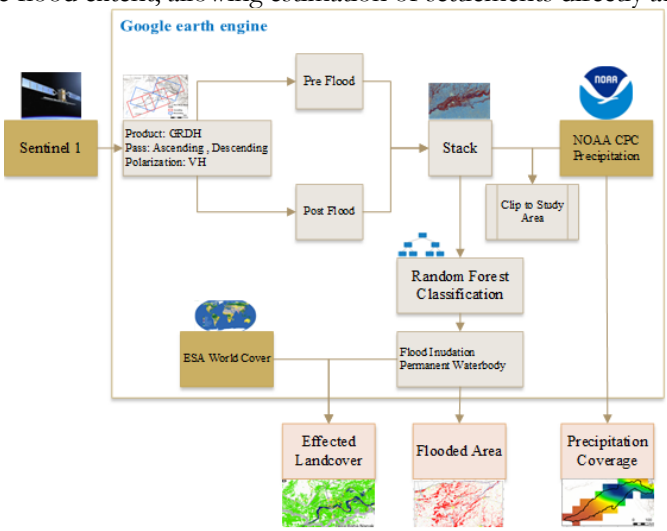

Figure 3. Flowchart of the methodology showing integration of Sentinel-1 SAR, NOAA CPC precipitation, and ESA WorldCover data in Google Earth Engine for flood mapping and land cover impact assessment.

The area of each class was calculated using Equation 1. The total area (A_c) of each class c(flooded extent, flooded agriculture, or flooded built-up land) was calculated by summing the product of a binary mask and the pixel area across the Ravi Basin. In this mask, $M_c(i)$equals 1 if pixel i belongs to class c, and 0 otherwise. Each pixel has a defined area P_i In m², which is later converted to km², and the summation is performed over all n pixels of the basin. The results were visualized in the GEE interface using custom palettes, and a user interface panel was added for interactive display of flood statistics and legend information. Finally, all intermediate and final outputs were exported from GEE for further analysis. Continuous rasters (e.g., pre- and post-flood backscatter and multi-band composites) were exported as 32-bit float images, whereas classified outputs were exported as 8-bit integer images to facilitate efficient storage and analysis.

$$A_c = \sum_{i=1}^{n} (M_c(i) \times P_i) \quad (1)$$

Precipitation Data:

To complement the flood mapping and validate the hydrometeorological drivers of the September 2025 flood, daily precipitation data were obtained from the NOAA CPC Global Unified Gauge-Based Precipitation dataset (mm/day) at 0.5° (~50 km) spatial resolution, available in Google Earth Engine. The dataset was filtered for February to September 2025, and precipitation statistics

(mean and standard deviation) were computed for each day using regional reduction over the study area geometry. A time series chart was produced for the entire basin, displaying temporal variations in rainfall intensity from February to September 10. Spatial precipitation patterns were derived by generating mean and standard deviation maps for August and September. These outputs provided a basin-wide perspective of rainfall variability and served as crucial supporting evidence to explain the severity and distribution of flooding observed in the Ravi Basin.

Results:

Flooded Region:

Figure 3 illustrates the spatial distribution of flood inundation within the Ravi Basin during the September 2025 event, as derived from Sentinel-1 SAR data. The composite map highlights inundated zones (in red), permanent waterbodies (in blue), and populated areas (in yellow), overlaid on the basin boundary. A series of inset maps (Figure 3B to F) provided detailed visualizations of flood impacts across critical locations. Panel B depicted the severe flooding in Dera Baba Nanak and Kartarpur, where floodwaters had encroached upon settlement areas and agricultural fields, submerging large territories of land. Similarly, panel F captures the western margins of Lahore city, where residential zones such as Theme Park and Park View experienced direct inundation, highlighting the exposure of even well-developed suburban sectors. Panel D emphasizes the widespread inundation south of Narowal, where built-up areas were directly intersected by floodwaters. Panels C and E further reveal flood penetration in the middle and lower Ravi floodplains, particularly near Pattoki and Gujranwala's adjoining settlements, confirming the river's floodplain vulnerability.

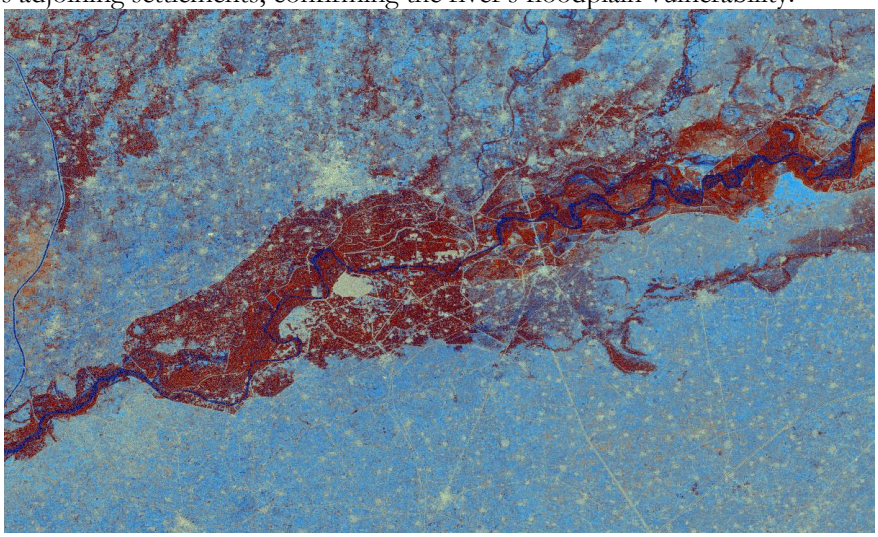

Figure 4. Sentinel-1 SAR composite showing flood-affected areas along the Ravi River, with inundated zones highlighted against surrounding land cover.

Figure 4 highlights the Chawinda–Zafarwal corridor, north of Narowal, which experienced some of the most extensive flooding during the event due to seasonal rivers. The figure highlights extensive inundation across croplands, with scattered villages and urban communities directly surrounded or submerged by floodwaters. Cyan markers represent settlements impacted, making it evident that flooding was not isolated to sparsely inhabited areas but extended into regions of dense habitation. The integration of OpenStreetMap data confirmed that approximately 260 settlements were affected basin-wide, ranging from small rural villages to larger towns. This number reflects the scale of socio-economic disruption, as most of these settlements rely heavily on agriculture and local trade that were compromised by prolonged inundation.

In terms of areal statistics, the results revealed that the total inundated area was 1,885.12 km², which represents 4.92% of the total basin area (38,305.89 km²). Agricultural land emerged as the most severely impacted category, with croplands in both upper and lower basin regions inundated, leading to direct livelihood losses for farming communities. Although built-up land covered a smaller proportion of the basin, it still experienced significant damage to bridges and roads, particularly around Narowal, Lahore's suburbs, and the urban fringes of Gujranwala District. The combined evidence from maps and settlement overlays confirms that flooding extended well beyond the main Ravi channel

into secondary distributaries and floodplain depressions, causing waterlogging, crop damage, and settlement disruption.

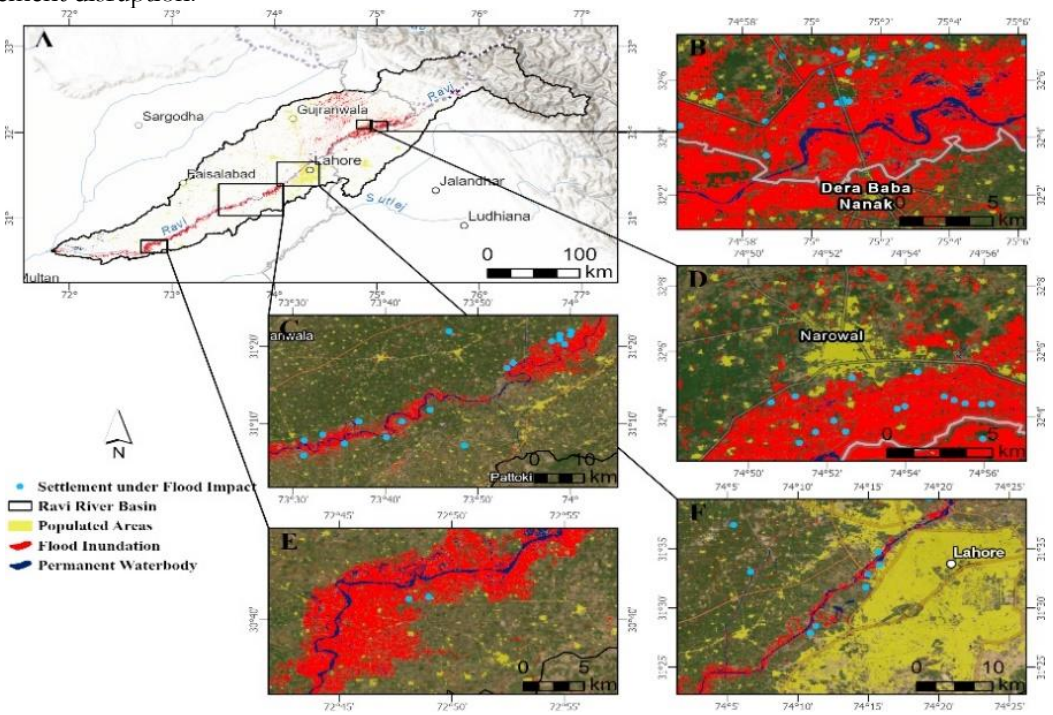

Figure 5. Flood inundation map of the Ravi River Basin during September 2025. Panels (B to F) show detailed views of major impacted zones.

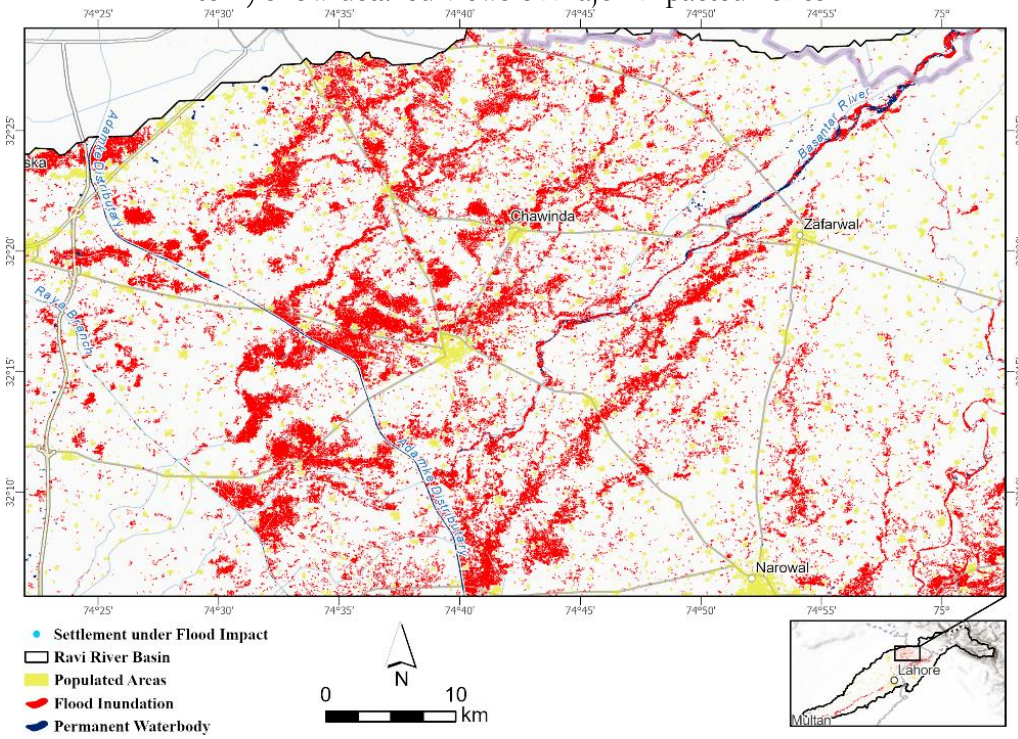

Figure 6. Flood inundation map of Chawinda and Zafarwal region within the Ravi Basin.

Affected Area:

Figure 5 illustrates the distribution of landcover classes within the Ravi Basin, highlighting their relation with the inundated areas during the September 2025 flood. The ESA WorldCover dataset was used to map key categories, including cropland, tree cover, shrubland, grassland, herbaceous wetlands, built-up areas, and sparse vegetation. Overlays of flood extent on land cover revealed that the impacts were uneven across classes, with certain land uses being disproportionately affected.

Quantitative analysis indicates that agriculture was the most severely affected class, with approximately 1,609.72 km² submerged out of a total agricultural area of 27,935.75 km² in the basin (Table 2). This demonstrates the severe agricultural losses, particularly across fertile floodplains in the middle and lower Ravi. Cropland near Jaranwala (Figure 5C) and Kamalia (Figure 5E) was among the worst affected, with extensive patches of standing crops inundated. Tree cover and grasslands were also notably affected, with about 51.42 km² of forested area and 90.21 km² of grassland inundated (Table 2). Tree cover losses are prominent near riparian corridors, while grasslands along the lower Ravi floodplains were inundated extensively. The impact on shrubland (22.34 km²) and sparse vegetation (62.87 km²) indicates that natural landscapes and semi-arid fringes of the basin were also exposed to waterlogging, though at a smaller scale compared to agricultural lands. Built-up areas experienced an inundation of 0.73 km² out of a total 2,501.77 km², though a small fraction at the basin level, but it has excessively high socio-economic consequences. Settlements like Narowal (Figure 5D), Dera Baba Nanak (Figure 5B), and towns of Lahore (Figure 5F) were directly affected, with household clusters submerged. Even small extents of flooding in built-up land correspond to significant population displacement and infrastructure damage. Herbaceous wetlands, though limited in total area within the basin, were also partially flooded (0.01 km² of 0.03 km²). While small in scale, this highlights that natural wetland ecosystems were not immune to the flooding dynamics.

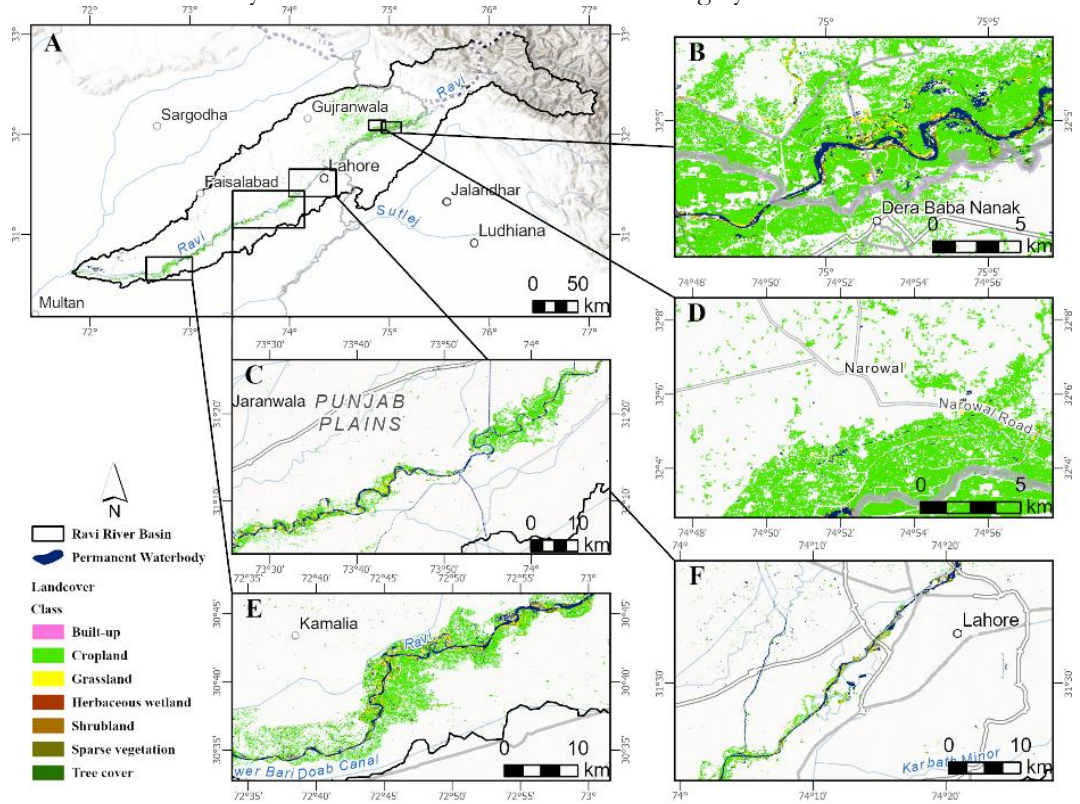

Figure 7. Land cover map of the Ravi Basin (A) with panels showing key areas (B to F).

Table 2. Flooded area and total land cover distribution within the Ravi Basin during the 2025 flood event.

Class	Flooded Area (km²)	Total Landcover Area (km²)	Affected (%)
Tree cover	51.42	7,776.39	0.66%
Shrubland	22.34	278.18	8.03%
Grassland	90.21	4,114.52	2.19%
Cropland	1,609.72	27,935.75	5.76%
Built-up	0.73	2,501.77	0.03%
Sparse vegetation	62.87	1,643.10	3.83%
Herbaceous wetland	0.01	0.03	33.33%

Overall, the findings confirm that the September 2025 flood was predominantly an agricultural disaster, with secondary impacts on natural vegetation and localized yet high-risk effects on settlements.

Precipitation Patterns

To investigate the meteorological drivers of the September 2025 flood, basin precipitation patterns were analyzed using NOAA CPC data. Figure 6 shows the spatial distribution of average precipitation and standard deviation (SD) across the Ravi Basin for the August and 10th September period. The average precipitation map reveals a strong spatial gradient, with the highest rainfall accumulations (up to 250 mm) concentrated in the northeastern basin, particularly over Sialkot and Narowal districts. This region, which forms the headwaters of several tributaries draining into the Ravi, recorded the most intense precipitation, consistent with reports of heavy monsoon rainfall during this period. In contrast, the southwestern basin received comparatively lower totals (28–80 mm). The precipitation variability showed 500 mm SD over the mean precipitation in the Sialkot Narowal corridor (Figure 6). Indicating recurrent and intense rainfall events within a short time frame. Such variability indicates extreme downpours mixed with moderate events, driving rapid runoff and intensifying downstream floods. The 2025 daily precipitation time series (Figure 7) further supports these observed patterns. The upper panel (blue bars) shows daily mean precipitation values, while the lower panel (red bars) highlights SD over mean precipitation events. A distinct surge in rainfall is visible from mid-August to early September, with peak daily totals exceeding 800 mm during late August. This timing coincided with the onset of widespread flooding in the basin. The temporal clustering of heavy rainfall, combined with its spatial concentration in the northeastern catchment, acted as the hydrological trigger for flood propagation downstream into the populated and agricultural areas of Lahore, Narowal, Gujranwala, and surrounding towns. Together, the spatial and temporal analyses establish that the September 2025 flood was primarily monsoon-driven, with the Sialkot–Narowal headwater zone acting as the epicenter of extreme precipitation.

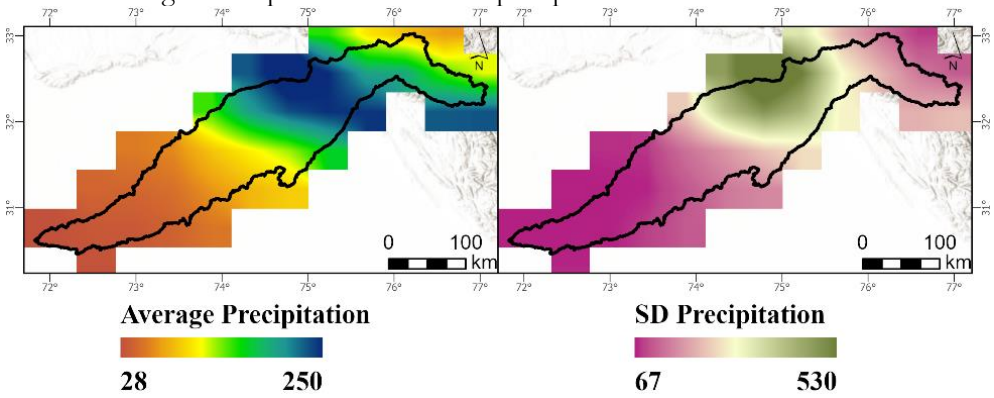

Figure 8. 1st August to 10th September average and standard deviation of precipitation across the Ravi Basin.

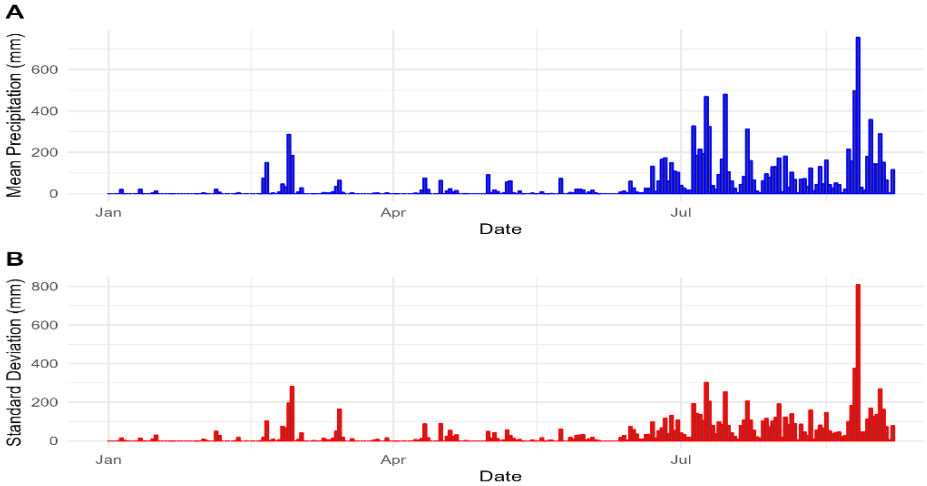

Figure 9. Daily precipitation patterns over the Ravi Basin showing temporal variability in 2025.

Discussion:

The September 2025 Punjab floods represent one of the most severe hydrological disasters in recent decades, both in terms of spatial extent and socio-economic consequences. Satellite-based analysis confirmed a total inundated area of 1,885.12 km², equivalent to 4.92% of the Ravi Basin, with approximately 260 settlements directly impacted. This remote sensing-derived evidence aligns closely with media reports highlighting the widespread inundation of villages and farmland [42][43]. According to DAWN News, more than 2.5 million people were displaced in Punjab, while approximately 100 lives were lost during the peak of the flood event [28]. The area's most severely affected included the eastern Punjab floodplains, with rivers Ravi, Sutlej, and Chenab overflowing simultaneously [27]. Reports have shown extensive submergence across districts such as Narowal and Gujranwala, while towns including Jalalpur Pirwala, Liaquatpur, and Lahore (Park View) were highlighted among those inundated [44][45]. This corresponds with our mapping outputs, which showed floodwater spreading beyond the main channel into agricultural corridors and urban fringes. The main cause was a combination of heavy monsoon rains and cross-border dam releases from India, which exacerbated already swollen rivers [44]. Precipitation analysis confirmed extreme rainfall clustering in the Sialkot and Narowal region, the same zone identified by media reports as the epicenter of rainfall-induced flooding (Figure 6). The combination of upstream inflows and local downpours accelerated flood propagation downstream into highly populated regions. The scale and severity of the event prompted several outlets to describe the floods as among the worst in decades for Punjab. It has been the 2nd time since 1988 that the flooding water reached up to bridges and some towns of Lahore [46]. Historical parallels can be drawn with the 2010 flood, which inundated one-fifth of Pakistan, and the 2014 Jhelum and Chenab floods, which had a similar tributary-driven characteristics [47][48]. However, what distinguishes 2025 is the simultaneous flooding of three major tributaries (Ravi, Sutlej, and Chenab), alongside the greater exposure of urban developments that were not majorly affected in earlier floods. Reports from neighboring basins highlighted widespread submergence of villages and cropland along the Sutlej and Chenab as well. Impacts were reported in the Sutlej Basin, where extensive submergence was observed in Bahawalnagar and Vehari districts, damaging cropland and displacing thousands of people [44][43]. Similarly, the Chenab Basin experienced major flooding across Multan, Jhang, and Jalalpur Pirwala, with reports noting the evacuation of over 25,000 people in Jalalpur Pirwala alone (NASA Earth Observatory, 2025; Reuters, 2025). While Ravi flooding was concentrated in Narowal and Gujranwala districts, the Sutlej and Chenab inundations spread further south into heavily cultivated floodplains. The September 2025 Punjab floods are expected to leave lasting consequences on Pakistan's economy and food systems well beyond the immediate disaster period. Punjab, known as the country's agricultural heartland, contributes a major share of national wheat, rice, and maize production. The flood inundation analysis confirmed that more than 1,600 km² of cropland was submerged, a finding consistent with media reports of extensive damage to standing rice and maize crops. With the flood striking just before the kharif harvest, large-scale crop losses are anticipated to reduce both household incomes and national grain stocks [46]. This shortfall could push food prices upward, intensifying inflationary pressures already present in the national economy. The livestock sector has also been disrupted, reporting loss of cattle and poultry in submerged villages, further affecting rural livelihood. Damage to transportation networks, markets, and irrigation infrastructure may also reduce agricultural output in subsequent seasons, compounding the initial losses. The humanitarian and economic consequences were immense. Relief operations faced significant challenges, including delayed evacuations, submerged road networks, and even boat capsizes during rescue missions [41]. On the policy side, the International Monetary Fund (IMF) announced that Pakistan's emergency flood spending and fiscal response will undergo review, highlighting the broader economic strain induced by the disaster [49].

Conclusion:

The September 2025 floods in Punjab represent a defining example of how monsoon variability and transboundary water dynamics combine to create large-scale disasters. Using Sentinel-1 SAR, this study mapped an inundated area of 1,885.12 km², equal to 4.92% of the Ravi Basin. The impacts were concentrated in croplands and settlements, with 1,609.72 km² of agriculture submerged and 260 settlements directly affected. Settlements such as Dera Baba Nanak, Kartarpur, and Lake City in Lahore demonstrate the expanding exposure of both rural and urban communities. Precipitation

analysis confirmed the Sialkot and Narowal belt as the rainfall epicenter, with daily peaks exceeding 800 mm. These findings align with news reports documenting over 2.5 million displaced persons and heavy crop and infrastructure losses. Beyond immediate impacts, the flood is expected to have a lasting impact on the Punjab economy and food security. Rice, maize, and livestock will reduce both household resilience and national grain stocks, while infrastructure damage may constrain production in subsequent seasons. The simultaneous flooding of three tributaries, Ravi, Sutlej, and Chenab, marks a significant shift from historic Indus-dominated floods. The study emphasizes the urgency of integrating SAR-based monitoring with precipitation forecasting, settlement mapping, and land-use planning. Ultimately, the 2025 Punjab flood serves as both a scientific case study and a warning of the vulnerabilities that lie ahead in a rapidly changing hydrological regime.

Reference:

[1] R. K. Mall, R. K. Srivastava, T. Banerjee, O. P. Mishra, D. Bhatt, and G. Sonkar, "Disaster Risk Reduction Including Climate Change Adaptation Over South Asia: Challenges and Ways Forward," *Int. J. Disaster Risk Sci.*, vol. 10, no. 1, pp. 14–27, Mar. 2019, doi: 10.1007/S13753-018-0210-9/FIGURES/2.

[2] V. Klemas, "Remote Sensing of Floods and Flood-Prone Areas: An Overview," *J. Coast. Res.*, vol. 31, no. 4, pp. 1005–1013, 2015, doi: https://doi.org/10.2112/JCOASTRES-D-14-00160.1.

[3] G. S. & K. S. Rawat, "Mapping flooded areas utilizing Google Earth Engine and open SAR data: a comprehensive approach for disaster response," *Discov. Geosci.*, vol. 2, no. 5, 2024, doi: https://doi.org/10.1007/s44288-024-00006-4.

[4] L. Wan, M. Liu, F. Wang, T. Zhang, and H. J. You, "Automatic extraction of flood inundation areas from SAR images: a case study of Jilin, China during the 2017 flood disaster," *Int. J. Remote Sens.*, vol. 40, no. 13, pp. 5050–5077, Jul. 2019, doi: 10.1080/01431161.2019.1577999.

[5] K. Jenkins, J. Hall, V. Glenis, and C. Kilsby, "A Probabilistic Analysis of Surface Water Flood Risk in London," *Risk Anal.*, vol. 38, no. 6, pp. 1169–1182, Jun. 2018, doi: 10.1111/RISA.12930.

[6] K. Calvin *et al.*, "IPCC, 2023: Climate Change 2023: Synthesis Report. Contribution of Working Groups I, II and III to the Sixth Assessment Report of the Intergovernmental Panel on Climate Change [Core Writing Team, H. Lee and J. Romero (eds.)]. IPCC, Geneva, Switzerland.," Jul. 2023, doi: 10.59327/IPCC/AR6-9789291691647.

[7] W. Solecki, D. Roberts, and K. C. Seto, "Strategies to improve the impact of the IPCC Special Report on Climate Change and Cities," *Nat. Clim. Chang.*, vol. 14, no. 7, pp. 685–691, Jul. 2024, doi: 10.1038/S41558-024-02060-9;SUBJMETA.

[8] S. S. J. T. Fasullo, B. L. Otto-Bliesner, "ENSO's Changing Influence on Temperature, Precipitation, and Wildfire in a Warming Climate," *Geophys. Res. Lett.*, 2018, doi: https://doi.org/10.1029/2018GL079022.

[9] N. J. & A. S. C. M. D. Flannigan, B. M. Wotton, G. A. Marshall, W. J. de Groot, J. Johnston, "Fuel moisture sensitivity to temperature and precipitation: climate change implications," *Clim. Change*, vol. 134, pp. 59–71, 2016, doi: https://doi.org/10.1007/s10584-015-1521-0.

[10] T. S. Ksiksi, T. Youssef, and E. Abdelmawla1, "Sea Level Rise and Abu Dhabi Coastlines: An Initial Assessment of the Impact on Land and Mangrove Areas," *J. Ecosyst. Ecography 2012 24*, vol. 2, no. 4, pp. 1–5, Aug. 2012, doi: 10.4172/2157-7625.1000115.

[11] P. B. Ashwini Kulkarni, T. P. Sabin, Jasti S. Chowdary, K. Koteswara Rao, P. Priya, Naveen Gandhi, "Precipitation Changes in India," *Assess. Clim. Chang. over Indian Reg. A Rep. Minist. Earth Sci. (MoES), Gov. India*, 2020, [Online]. Available: https://link.springer.com/chapter/10.1007/978-981-15-4327-2_3

[12] Q. Z. C. Rasul, Ghulam Dahe, Qin, "GLOBAL WARMING AND MELTING GLACIERS ALONG SOUTHERN SLOPES OF HKH RANGES," *Pakistan J. Meteorol.*, vol. 5, no. 9, 2005, [Online]. Available: https://www.pmd.gov.pk/rnd/rnd_files/vol5_issue9/6.Global Warming and Melting Glaciers along Southern Slopes of HKH Ranges.pdf

[13] "UAE rains: Municipality worker drowns after tanker swept away by floodwaters in Al Dhaid region." Accessed: Oct. 04, 2025. [Online]. Available: https://gulfnews.com/uae/emergencies/uae-rains-municipality-worker-drowns-after-tanker-swept-away-by-floodwaters-in-al-dhaid-region-1.102251666

[14] A. Bijalwan, S. L. Swamy, C. M. Sharma, N. K. Sharma, and A. K. Tiwari, "Land-use, biomass and carbon estimation in dry tropical forest of Chhattisgarh region in India using satellite remote sensing and GIS," *J. For. Res.*, vol. 21, no. 2, pp. 161–170, Jun. 2010, doi: 10.1007/S11676-010-0026-Y/METRICS.

[15] S. T. Varun Tiwari , Vinay Kumar, Mir Abdul Matin, Amrit Thapa, Walter Lee Ellenburg, Nishikant Gupta, "Flood inundation mapping- Kerala 2018; Harnessing the power of SAR, automatic threshold detection method and Google Earth Engine," *PLoS One*, 2020, doi: https://doi.org/10.1371/journal.pone.0237324.

[16] A. K. Agnihotri, A. Ohri, S. Gaur, Shivam, N. Das, and S. Mishra, "Flood inundation mapping and monitoring using SAR data and its impact on Ramganga River in Ganga basin," *Environ. Monit. Assess.*, vol. 191, no. 12, pp. 1–16, Dec. 2019, doi: 10.1007/S10661-019-7903-4/METRICS.

[17] M. A. Aziz *et al.*, "Delineating Flood Zones upon Employing Synthetic Aperture Data for the 2020 Flood in Bangladesh," *Earth Syst. Environ.*, vol. 6, no. 3, pp. 733–743, Sep. 2022, doi: 10.1007/S41748-022-00295-0/METRICS.

[18] V. Chauhan and J. Dixit, "Fractal analysis of major faults and fractal dimension of lineaments in the Indo-Gangetic Plain on a regional scale," *Earthq. Sci.*, vol. 37, no. 2, pp. 107–121, 2024, [Online]. Available: https://doi.org/10.1016/j.eqs.2024.01.015

[19] Q. M. Muhammad Rizwan, Xin Li, Yingying Chen, Lubna Anjum, Shanawar Hamid, Muhammad Yamin, Junaid Nawaz Chauhdary, Muhammad Adnan Shahid, "Simulating future flood risks under climate change in the source region of the Indus River," *J. Flood Risk Manag.*, 2022, doi: https://doi.org/10.1111/jfr3.12857.

[20] T. E. F. and F. P. Stephanie Long, "Flood extent mapping for Namibia using change detection and thresholding with SAR," *Environ. Res. Lett.*, vol. 9, no. 3, 2014, doi: 10.1088/1748-9326/9/3/035002.

[21] J. R. C. & M. W. Caroline Taylor, Tom R. Robinson, Stuart Dunning, "Glacial lake outburst floods threaten millions globally," *Nat. Commun.*, vol. 14, no. 487, 2023, doi: https://doi.org/10.1038/s41467-023-36033-x.

[22] D. B. C. S. V. Anand Shankar, Ashish Kumar Sinha, "A Case Study of Heavy Rainfall Events and Resultant Flooding During the Summer Monsoon Season 2020 Over the River Catchments of North Bihar, India," *VayuMandal*, vol. 48, no. 2, 2022, [Online]. Available: https://imetsociety.org/wp-content/pdf/vayumandal/2022482/2022482_7.pdf

[23] K. Uddin, M. A. Matin, and F. J. Meyer, "Operational Flood Mapping Using Multi-Temporal Sentinel-1 SAR Images: A Case Study from Bangladesh," *Remote Sens. 2019, Vol. 11, Page 1581*, vol. 11, no. 13, p. 1581, Jul. 2019, doi: 10.3390/RS11131581.

[24] J. Wang *et al.*, "Disaster mapping and assessment of Pakistan's 2022 mega-flood based on multi-source data-driven approach," *Nat. Hazards*, vol. 120, no. 4, pp. 3447–3466, Mar. 2024, doi: 10.1007/S11069-023-06337-8/METRICS.

[25] "Pakistan issues flood warnings for Ravi, Sutlej rivers as monsoon death toll nears 800 | Arab News." Accessed: Oct. 04, 2025. [Online]. Available:

https://www.arabnews.com/node/2612940/amp
[26] "BBC Lancashire on X: "'My family escaped Pakistan flooding just in time" https://t.co/pGD6frNGgF' / X." Accessed: Oct. 04, 2025. [Online]. Available: https://x.com/BBCLancashire/status/1962539392242774208
[27] "Home - FFD Lahore." Accessed: Oct. 04, 2025. [Online]. Available: https://ftp.pmd.gov.pk/home
[28] "NDMA issues high-flood alert for Ravi as India releases water - Pakistan - DAWN.COM." Accessed: Oct. 04, 2025. [Online]. Available: https://www.dawn.com/news/1937340
[29] E. Özelkan, "Water Body Detection Analysis Using NDWI Indices Derived from Landsat-8 OLI," *Polish J. Environ. Stud.*, vol. 29, no. 2, pp. 1759–1769, 2020, doi: https://doi.org/10.15244/pjoes/110447.
[30] B. A. B. Chandrababu Naik, "Extraction of Water-body Area from High-resolution Landsat Imagery," *Int. J. Electr. Comput. Eng.*, vol. 8, no. 6, p. 12, 2018, [Online]. Available: https://ijece.iaescore.com/index.php/IJECE/article/view/11740
[31] A. Tarpanelli, A. C. Mondini, and S. Camici, "Effectiveness of Sentinel-1 and Sentinel-2 for flood detection assessment in Europe," *Nat. Hazards Earth Syst. Sci.*, vol. 22, no. 8, pp. 2473–2489, Aug. 2022, doi: 10.5194/NHESS-22-2473-2022.
[32] O. S. Yilmaz, F. Gulgen, F. Balik Sanli, and A. M. Ates, "The Performance Analysis of Different Water Indices and Algorithms Using Sentinel-2 and Landsat-8 Images in Determining Water Surface: Demirkopru Dam Case Study," *Arab. J. Sci. Eng.*, vol. 48, no. 6, pp. 7883–7903, Jun. 2023, doi: 10.1007/S13369-022-07583-X/METRICS.
[33] G. Nico, M. Pappalepore, G. Pasquariello, A. Refice, and S. Samarelli, "Comparison of SAR amplitude vs. coherence flood detection methods - a GIS application," *Int. J. Remote Sens.*, vol. 21, no. 8, pp. 1619–1631, Jan. 2000, doi: 10.1080/014311600209931.
[34] T. A. Mohammed Siddique, "CCD-Conv1D: A deep learning based coherent change detection technique to monitor and forecast floods using Sentinel-1 images," *Remote Sens. Appl. Soc. Environ.*, vol. 37, p. 101440, 2025, doi: https://doi.org/10.1016/j.rsase.2024.101440.
[35] B. I. Hassan Ait Naceur, "Machine learning-based optimization of flood susceptibility mapping in semi-arid zone," *DYSONA - Appl. Sci.*, 2025, [Online]. Available: https://applied.dysona.org/article_209038.html
[36] Y. J. Yi Liu, "Convolutional Neural Network-Based Machine Vision for Non-Destructive Detection of Flooding in Packed Columns," *Sensors*, vol. 23, no. 5, p. 2658, 2023, doi: https://doi.org/10.3390/s23052658.
[37] M. M. Khuong H. Tran, "Surface Water Mapping and Flood Monitoring in the Mekong Delta Using Sentinel-1 SAR Time Series and Otsu Threshold," *Remote Sens*, vol. 14, no. 22, p. 5721, 2022, doi: https://doi.org/10.3390/rs14225721.
[38] "Rapid attribution of heavy rainfall events leading to the severe flooding in Western Europe during July 2021 - Zurich Climate Resilience Alliance." Accessed: Oct. 04, 2025. [Online]. Available: https://zcralliance.org/resources/item/rapid-attribution-of-heavy-rainfall-events-leading-to-the-severe-flooding-in-western-europe-during-july-2021/
[39] J. Liang and Desheng Liu, "A local thresholding approach to flood water delineation using Sentinel-1 SAR imagery," *ISPRS J. Photogramm. Remote Sens.*, vol. 159, pp. 53–62, 2020, doi: https://doi.org/10.1016/j.isprsjprs.2019.10.017.
[40] A. T. Hamid Gulzar, Sajid Ghuffar, Syed Amer Mahmood, Saif Ullah Akhter, Hania Arif, Dmitry E. Kucher, "Assessment of land deformation and groundwater depletion using Sentinel-1 PS InSAR, GRACE, and Borehole data," *Remote Sens. Appl. Soc. Environ.*, vol. 39, p. 101639, 2025, doi: https://doi.org/10.1016/j.rsase.2025.101639.

[41] "Pakistan: More than two million evacuated from deadly floods." Accessed: Oct. 04, 2025. [Online]. Available: https://www.bbc.com/news/articles/cn0xjd7wvy1o

[42] "Monsoon Rains Flood Pakistan." Accessed: Oct. 04, 2025. [Online]. Available: https://earthobservatory.nasa.gov/images/154781/monsoon-rains-flood-pakistan

[43] "'Everything is gone': Punjabi farmers suffer worst floods in three decades | India | The Guardian." Accessed: Oct. 04, 2025. [Online]. Available: https://www.theguardian.com/world/2025/sep/06/everything-gone-punjabi-farmers-suffer-worst-floods-three-decades

[44] "Mass evacuations in Pakistan's flooded Punjab hit 300,000 in 48 hours | Climate Crisis News | Al Jazeera." Accessed: Oct. 04, 2025. [Online]. Available: https://www.aljazeera.com/news/2025/9/3/mass-evacuations-in-pakistans-flooded-punjab-hit-300000-in-48-hours

[45] "Watch: Luxury neighbourhood in Lahore submerged in floods." Accessed: Oct. 04, 2025. [Online]. Available: https://www.bbc.com/news/videos/cm2vdm1pnd8o

[46] "Five Lahore localities flooded by the Ravi - Pakistan - DAWN.COM." Accessed: Oct. 04, 2025. [Online]. Available: https://www.dawn.com/news/1938079

[47] S. F. . Yuneng Du, Luan Jingdong, Rafia Khatoon, "Flood Disaster in Pakistan and its Impact on Agriculture Growth (A Review)," *Glob. Adv. Res. J. Agric. Sci.*, vol. 4, no. 12, 2015, [Online]. Available: https://www.researchgate.net/publication/286879062_Flood_Disaster_in_Pakistan_and_its_Impact_on_Agriculture_Growth_A_Review

[48] S. H. Muhammad Junaid Siddiqui, "Rainfall–runoff, flood inundation and sensitivity analysis of the 2014 Pakistan flood in the Jhelum and Chenab river basin," *Hydrol. Sci. J.*, vol. 63, no. 13–14, pp. 1976–1997, 2018, doi: ps://doi.org/10.1080/02626667.2018.1546049.

[49] "IMF team to assess flood spending later this month - Business - DAWN.COM." Accessed: Oct. 04, 2025. [Online]. Available: https://www.dawn.com/news/1942071